CHAPTER 2

BASIC PRINCIPLES

In present, fuel cell had been mentioned frequently cause of Global Warming problems and the increasing price of gasoline. However, it is a refresh technology and not enough widespread information. This chapter will introduce the principles of fuel cell basis; especially for proton exchange membrane (PEM) fuel cell, the principles of plasma enhanced coating using in this research and coating characterization principles.

2.1 Fuel cell basic

A fuel cell is an electrochemical energy converter that converts chemical energy of fuel directly into direct current (DC) electricity without involving any moving parts. A fuel cell is in some aspects similar to a battery. It has an electrolyte, and negative and positive electrodes and it generates DC electricity through electrochemical reactions. However, unlike a battery, a fuel cell requires a constant supply of fuel and oxidant. Also, unlike in a battery, the electrodes in a fuel cell do not undergo chemical changes. Batteries generate electricity by the electrochemical reactions that involve the materials that are already in batteries. Because of this, a battery may be discharged, which happens when the materials that participate in the electrochemical reactions are depleted. A fuel cell cannot be discharged as long as the reactants – fuel and oxidant -- are supplied. Another difference between a fuel cell and a battery is that a fuel cell generates by-products: waste heat and water, and the system is required to manage those (a battery also generates some heat but at a much lower rate that usually does not require any special or additional equipment).

2.1.1 Proton exchange membrane fuel cell

Fuel cells can be grouped by the type of electrode they use. Proton exchange membrane or polymer electrolyte membrane fuel cell (PEMFC) use a thin (≤50 μm) proton conductive polymer membrane (such as perfluorosulfonated acid polymer) as the electrolyte. The catalyst is typically platinum supported on carbon with loadings of about 0.3 mg/cm^2. Operating temperature is typically between 60 and 80 ˚C. PEM fuel cells are a serious candidate for automotive applications, but also for small-scale distributed stationary power generation, and for portable power applications as well.

A cross-sectional diagram of a single cell is shown in Figure 2.1. The proton exchange membrane is in contact with the anode catalyst layer (show on the left) and the cathode catalyst layer (show on the right). Each catalyst layer is in contact with a gas diffusion layer. The membrane, catalyst layers, and the gas diffusion layers make up are called the membrane-electrode-assembly (MEA).

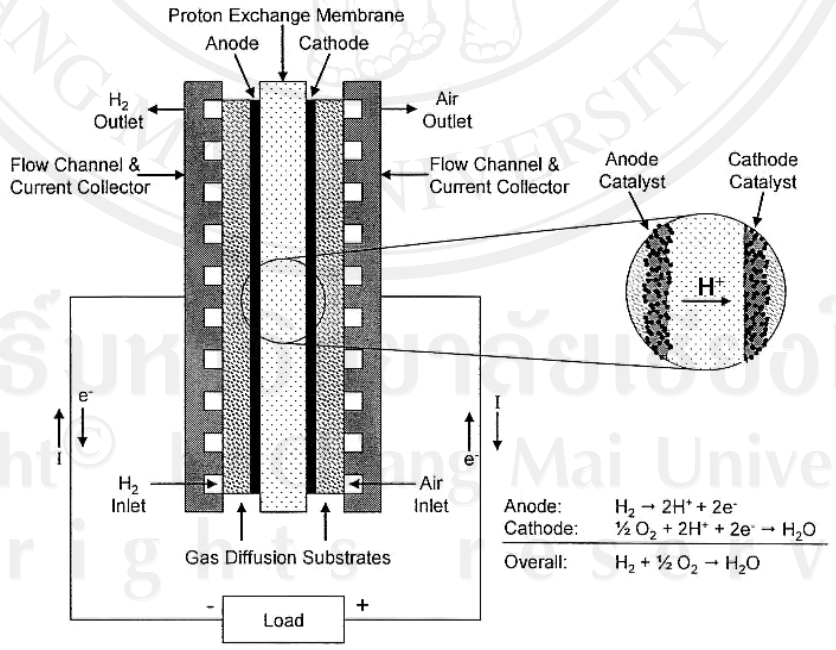

Figure 2.1 Cross section of a proton exchange membrane fuel cell (Cooper et al., 2005).

Fuel in form of hydrogen gas is fed into the anode side of the PEM fuel cell. The oxidant in a fuel cell is oxygen, either in air or as a pure gas, which enters the fuel cell through the cathode inlet. The reactant gases flow through channels and migrate through gas diffusion layers to the catalyst surface on their respective sides of the MEA. Aided by the noble metal catalyst in the anode, hydrogen is oxidized to form protons and electrons. The proton move through the proton exchange membrane and the electrons travel from the anode through an external circuit (thereby causing a flow of electric current) to the cathode. At the cathode catalyst layer, oxygen combines with the protons that pass through the membrane and the electrons that travel through the external circuit to form water and heat.

The electrochemical reactions in fuel cells happen simultaneously on both side of the membrane; the anode and the cathode. The basic fuel cell reactions are:

At the anode:

$$H_2 \rightarrow 2H^+ + 2e^- \quad . \tag{2.1}$$

At the cathode:

$$\frac{1}{2}O_2 + 2H^+ + 2e^- \rightarrow H_2O \quad . \tag{2.2}$$

Overall:

$$H_2 + \frac{1}{2}O_2 \rightarrow H_2O \quad . \tag{2.3}$$

These reactions may have several intermediate steps, and there may be some side reactions, but these reactions accurately describe the main processes in a cell.

The standard theoretical or ideal potential (E^0_{theor}) for H_2/O_2 cell reaction is determined from the change in Gibbs free energy (ΔG^0) for the reaction at unit activity of all reactants and products,

$$E^0_{theor} = -\frac{\Delta G^0}{n.F} \quad , \tag{2.4}$$

where n is the number of electron required to complete the reaction (n = 2 equivalent/mole H_2) and F is Faraday's constant (96,485 Coulombs/equivalent).

The change in Gibbs free energy at 25 °C for reaction equation (2.3) is -237.3 kJ/mole assuming liquid water product, and -228.1 kJ/mole assuming vapor water product. Appling equation (2.1) the corresponding E^0_{theor} values are 1.23 V and 1.18 V, respectively. However, the change in Gibbs free energy in reaction equation (2.3) is a function of temperature and the form of reaction product. To calculate the standard theoretical cell potential at any temperature, ΔG^0 must be calculated at that temperature. The standard Gibbs free energy change for reaction equation (2.3) assuming water vapor reaction product are published in the International Critical Tables of Numerical Data, Physics, Chemistry and Technology (Washburn, 2003),

$$\Delta G^0 = -240{,}203 + 3.933 \cdot T \cdot \ln(T) + 0.0069 \cdot T^2 - 1.54808 \times 10^{-6} \cdot T^3 + 16.40 \cdot T \quad , \qquad (2.5)$$

where ΔG^0 is in Joules per mole (J/mole) and T is in K. equations (2.4) and (2.5) are used to calculate the theoretical cell potential at any temperature under unit activity conditions.

At non-standard conditions, the Nernst equation is used to calculate the theoretical cell voltage (E_{theor}). Equation (2.6) is the Nernst equation specifically written for the H_2/O_2 cell,

$$E_{theor} = E^0_{theor} + \left(\frac{R \cdot T}{n \cdot F}\right) \ln\left(\frac{(p_{H_2}) \cdot (p_{O_2})^{1/2}}{p_{H_2O}}\right) \quad , \qquad (2.6)$$

where

E_{theor} = theoretical cell voltage at non-standard concentrations and at temperature T, volts

E^0_{theor} = theoretical cell voltage at standard concentrations and at temperature T, volts

R = gas constant, 8.314 Joule/mole K

T = temperature, K

F = Faraday's constant, 96485 C/equivalent

n = moles of electrons produced per mole of H_2 reacted (n = 2 for this reaction), equivalent/mole

p_{H2}, p_{O2}, p_{H2O} = partial pressures of H_2, O_2 and H_2O, respectively, atm

The Nernst equation indicates that the theoretical cell voltage is a logarithmic function of the H_2 partial pressure, the square root of the O_2 partial pressure and the inverse of the water partial pressure. It is evident that increasing the pressure or concentration of reactants will increase E_{theor} whereas decreasing their concentration will reduce E_{theor}.

Equations (2.4) through (2.6) are used to calculate the theoretical potential of the fuel cell at non-standard conditions. The standard potential for the H_2/O_2 cell is indicated on the current density-voltage diagram in Figure 2.2 as the horizontal line drawn at a voltage of 1.18 V.

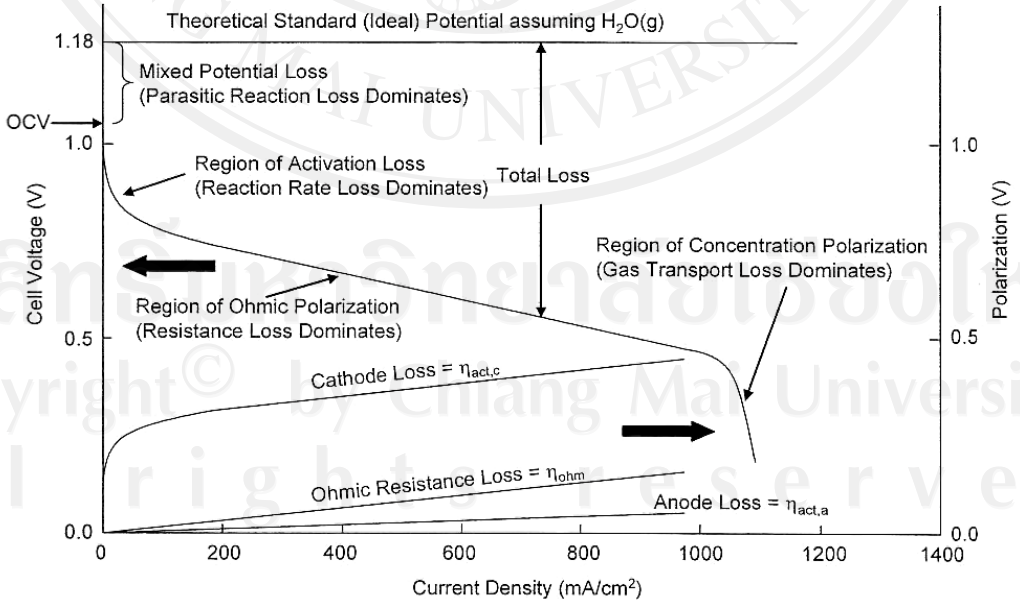

Figure 2.2 Representative fuel cell performance curves at 25 °C, 1 atm (Cooper et al., 2005).

When an external resistance, referred as a “load”, is applied to the cell, non-equilibrium exists and a net current flows through the load. The net rate of an electrochemical reaction is proportional to the current density. The cell voltage becomes smaller as the net reaction rate increase because of irreversible loses. Sources of voltage loss (polarization, η) shown in Figure 2.2 are:

i) Activation of the electrode reaction, dominate at the low current density regime.

ii) Ohmic resistance, dominate in the mid-current range.

iii) Transport limitation, dominate at high currents.

Deviations between the reversible potential and the polarization curve provide a measure of fuel cell efficiency. Fuel cell efficiency can be defined as several ways. In an energy-producing process such as fuel cell, current efficiency (ε_i) is defined as,

$$\varepsilon_i = \frac{\text{Actual current produced}}{\text{Theoretical current that should be produced for agiven reactant feed rate}} \tag{2.7}$$

For the stoichiometric ratio of 1 (100 % utilization) and negligible loss of reactant, the current efficiency can be taken as 100%.

Voltage efficiency (ε_v) is defined as,

$$\varepsilon_v = \frac{\text{Actual cell voltage}}{\text{Theoretical cell voltage}} = \frac{E_{cell}}{E_{theor}} \tag{2.8}$$

The total chemical energy of a fuel cell reaction is given by the change of enthalpy of the reaction. If all of the chemical energy could generate electricity, the cell voltage would be 1.48 V base on the heat of formation of liquid water at standard conditions. This value is referred to as the thermo-neutral potential. However, only the change in Gibbs free energy actually contributes to the theoretical cell voltage. The difference between these two quantities is energy that is liberated as waste heat. This effect establishes a maximum possible efficiency (ε_{max}) equal to,

$$\varepsilon_{\max} = \frac{\text{Theoretical cell voltage}}{\text{Thermoneutral potential}} = \frac{1.23}{1.48} = 0.83@25^{\circ}C \qquad (2.9)$$

Note that because the theoretical cell voltage is a function of temperature (Eq. (2.4) to (2.6)), so is ε_{max}.

Finally, the overall energy efficiency (ε_e) can be defined as the product of the current, voltage, and maximum efficiencies,

$$\varepsilon_e = \varepsilon_i \cdot \varepsilon_V \cdot \varepsilon_{\max} \qquad (2.10)$$

The power density delivered by a fuel cell is the product of the current density and the cell voltage at that current density,

$$\text{Power density}\,(\text{W/cm}^2) = \text{i} \cdot \text{V} \qquad (2.11)$$

Power density is a non-linear function of current density and typically is maximized at approximately 2/3 of the limiting current density.

2.1.2 Fuel cell bipolar plates

The two plates on each side of the membrane electrode assembly are called bipolar plates. The fully functioning bipolar plates are essential for multi cell configurations as shown in Figure 2.3, by electrically connecting the anode of one cell to the cathode of the adjacent cell.

The bipolar collector/separator plates have several functions in a fuel cell stack. Cooper et al. (2005) elucidated a number of properties desirable in a bipolar plate, namely:

- They connect cells electrically in series – therefore, they must be electrically conductive.

- They separate the gases in adjacent cells – therefore, they must be impermeable to gases.

- They provide structural support for the stack – therefore, they must have adequate strength, yet they must be lightweight.

- They conduct heat from active cells to the cooling cells or conduits – therefore, they must be thermally conductive.

- They typically house the flow field channels – therefore, they must be conformable.

In addition, they must be corrosion resistant in the fuel cell environment, yet they must not be made out of "exotic" and expensive materials. To keep the cost down not only must be inexpensive material, but also the manufacturing process must be suitable for mass production.

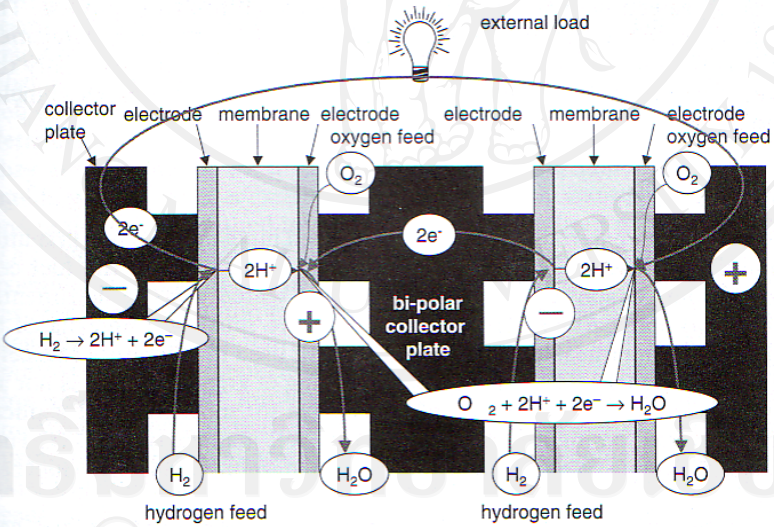

Figure 2.3 Bipolar plate connects and separates two adjacent cells (Cooper et al., 2005).

Some of the above mentioned requirements may contradict each other; therefore, selection of the material involves an optimization process. The resulting material may not be the best one in any of the property categories, but it is the best

one which satisfies the optimization criteria (typically the lowest cost per kWh of electricity produced).

Metals, as sheets, are potential candidates for bipolar plate material (Hermann et al., 2005) since they have good mechanical stability, electrical conductivity and thermal conductivity and can be easily stamped to desired shape to accommodate the flow channels. However, as bipolar plates are exposed to an operating environment with a pH of 2–3 at temperatures of around 80 ºC, metal plates are prone to corrosion or dissolution. The dissolved metal ions may lead to poisoning of PEM membrane and hence lowering of ionic conductivity. Moreover, a corrosion layer on the surface of a bipolar plate increases the electrical resistance and decreases the output of the cell. Due to this these issues, the metal bipolar plate need to be coated with a protective layer.

Recent studies by Wang et al. (2003; 2004) at the National Renewable Energy Laboratory, Golden (USA) show that stainless steel is a strong candidate for bipolar plate material. However, to avoid corrosion, metallic bipolar plates are coated with protective coating layers. Coatings should be conductive and adhere to the base metal without exposing it. Further the coefficient of thermal expansion of the base metal and the coating should be as close as possible to eliminate the formation of micro-pores and micro-cracks in coatings due to unequal expansion. There are two types of coatings, carbon-based and metal-based (Mehta and Cooper, 2003). Noble metals, metal nitrides and metal carbides are some of the metal-based coatings.

2.2 Principle of plasma processing

The term plasma was apparently by Irving Langmuir in 1929 (Langmuir, 1929) to describe the behavior of ionized gases in high current vacuum tubes. It was realized that plasmas exhibited a behavior different from simple un-ionized gases. Plasmas were termed a rare fourth state of matter. There are many plasma processing operations used for surface coating. This part is to introduce fundamental of cathodic arc, plasma nitriding and sputtering.

2.2.1 Cathodic arc

The cathodic arc has the same meaning as the vacuum arc, but the cathodic arc occurred at elevated gas pressure and the gas participated significantly in the discharge process. Nevertheless, the term “cathodic arc” and “vacuum arc” often correctly used interchangeably (Pasaja, 2008).

Vacuum arc is a plasma discharge that takes place between two metallic electrodes (cathode and anode) in vacuum (Brown, 1994). Ionization process can occur at both cathode and anode surface, if ionization process occurs at cathode surface it is called *cathodic arc* whereas if plasma ions are not generated from cathode material but at anode surface it is called *anodic arc*. The cathodic arc is mostly used in most application because of there efficiently production of metal plasma and its simplicity. These are basic features that make it well suited for film deposition application. Cathodic arc can operate in both pulsed and DC or continuous mode. The pulsed cathodic arc was used in this experiment. The advantage of pulsed operation is mainly related to the significant reduction requirement of good cooling.

Most common for pulsed cathodic arc sources are high-voltage surface flashovers triggering (Brown, 1994) and low-voltage “triggerless” arc initiation (Anders et al., 1998; 1999). High voltage pulse is requires for trigger electrode that is separated from the cathode by an insulating spacer (Figure 2.4(a)). Whereas relatively low voltage is requires for triggerless arc initiation. A conductive coating, preferably of the cathode material, is deposited on the insulator separating cathode and anode (Figure 2.4(b)). When the arc supply voltage is applied, which is typically one hundred to several hundred volts, plasma is formed at the interface between the coating and the cathode due to joule ohmic heating. This method has very simple and very reliable for most cathode materials. An arc power supply for triggering operation is based on a thyristor-switched pulsed forming network (Anders et al., 1999).

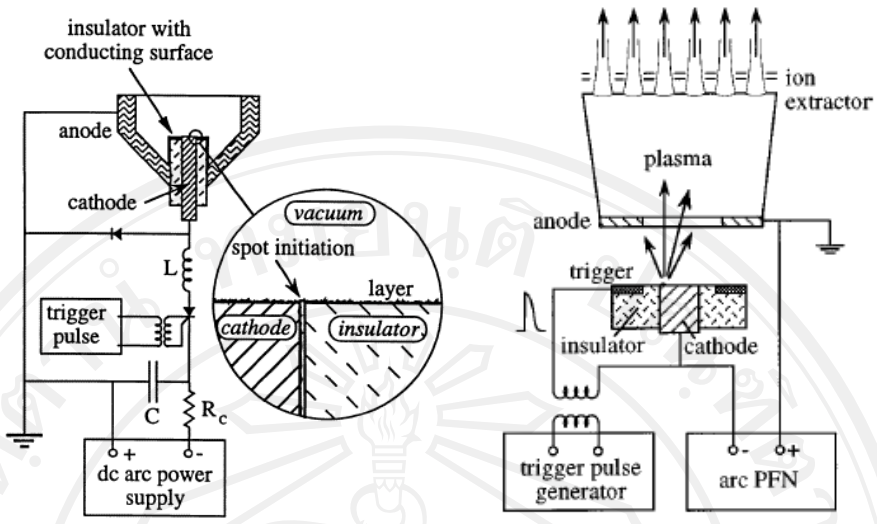

(a) (b)

Figure 2.4 (a) A conventional cathodic arc source. (b) A repetitively "triggerless" cathodic arc source (Anders et al., 1999).

2.2.2 Plasma nitriding

Plasma nitriding or 'ion' nitriding (sometimes also called plasma ion nitriding) or glow-discharge nitriding, is an industrial surface hardening treatment for metallic materials (plasma nitriding from Wikipedia, 2009). A plasma is the 'fourth' state of matter, the other three being solid, liquid and gaseous states. In the plasma state, matter exists in its excited form, also called the 'ionized' form, meaning the electrons in the outermost orbit have been knocked off. Thus plasma usually is an ionized gas, and a mixture of neutral as well as charged particles. There are hot plasmas typified by plasma jets used for metal cutting, welding, cladding or spraying. There are also cold plasmas, usually generated inside vacuum chambers, at low pressure regimes. Here the high temperature characteristics of the ionized gases are not used, but the electronic properties become more useful. Thus an ionized gas like nitrogen in such a low pressure regime becomes much more reactive. Thus surface treatment using the ionized nitrogen results in hardening of metals by two mechanisms: by diffusion, since the diffusivity of the excited nitrogen atoms is higher -can be up to ten times faster compared with gas nitriding, forming the *Diffusion Zone* where precipitation

hardening is present, and by thermo-chemical reactions which yield a thin layer of very hard iron and alloy nitrides, named *Compound Layer* or *White Layer*. Usually steels, alloy steels etc. are very beneficially treated with plasma nitriding.

Plasma nitrocarburizing is in essence a variant of well-established plasma nitriding method. It is a physical and a thermal–chemical process in which the nitrogen and carbon atoms diffuse into the workpiece surface simultaneously around the eutectoid temperature (565 $^{\circ}$C) of Fe–C–N diagram. Nitrocarburizing possesses advantages of shorter treatment time than gas nitriding, lower adhesion wear of the coated layer and it can be applied in a variety of steels. The plasma nitrocarburizing is superior to the conventional gas nitrocarburizing, because the bombardment of the carbon and nitrogen ions on the surface of the work can virtually depassivate the film of chromium oxide of the stainless steels, as a consequence it can be applied to nitrocarburize the stainless steel without difficulty. Furthermore, the plasma nitrocarburizing can easily control the ingredient of the compound layer by adjusting the composition of the atmosphere. Generally, plasma nitrocarburizing was conducted in an atmosphere of N_2/H_2 with addition of CH_4 by an intensified glow-discharge. The surface of stainless steel is continuously subjected to a highly energized ions flux for removing the oxide films by the sputtering actions, the nitrogen and carbon atoms diffusing into the substrate to form compound layer at the same time. Chang and Chen (2003) shown that by this technique, N atom can penetrated up to 70 μm into the steel as shown in Figure 2.5.

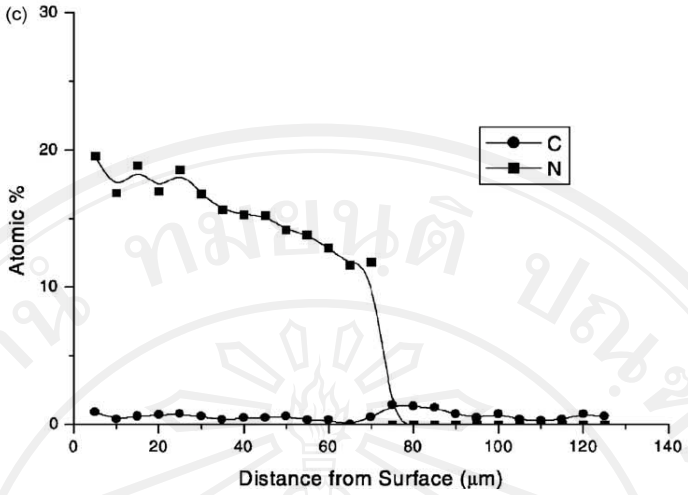

Figure 2.5 C and N elements near the surface of the specimen nitrocarburized in the mixture gas of N_2/H_2 = 4/1 with 2% CH_4 addition, at 570 °C, 560 Pa for 5 h (Chang and Chen, 2003).

2.2.3 Magnetron sputtering

Magnetron sputtering is a powerful and flexible technique which can be used to coat virtually any workpiece with a wide range of materials; any solid metal or alloy and a variety of compounds. Sputtering is the removal of atomic material from a solid due to energetic bombardment of its surface layers by ions or neutral particles.

Prior to the sputtering procedure a vacuum of less than one ten millionth of an atmosphere must be achieved. From this point a closely controlled flow of an inert gas such as argon is introduced. This raises the pressure to the minimum needed to operate the magnetrons, although it is still only a few ten thousandth of atmospheric pressure.

When power is supplied to a magnetron a negative voltage of typically -300V or more is applied to the target. This negative voltage attracts positive ions to the target surface at speed. Generally when a positive ion collides with atoms at the surface of a solid an energy transfer occurs. If the energy transferred to a lattice site is

greater than the binding energy, primary recoil atoms can be created which can collide with other atoms and distribute their energy via collision cascades. A surface atom becomes sputtered if the energy transferred to it normal to the surface is larger than about 3 times the surface binding energy (approximately equal to the heat of sublimation).

Sputtering of a target atom is just one of the possible results of ion bombardment of a surface. The other possibilities are summarized in Figure 2.6. Aside from sputtering the second important process is the emission of secondary electrons from the target surface. These secondary electrons enable the glow discharge to be sustained.

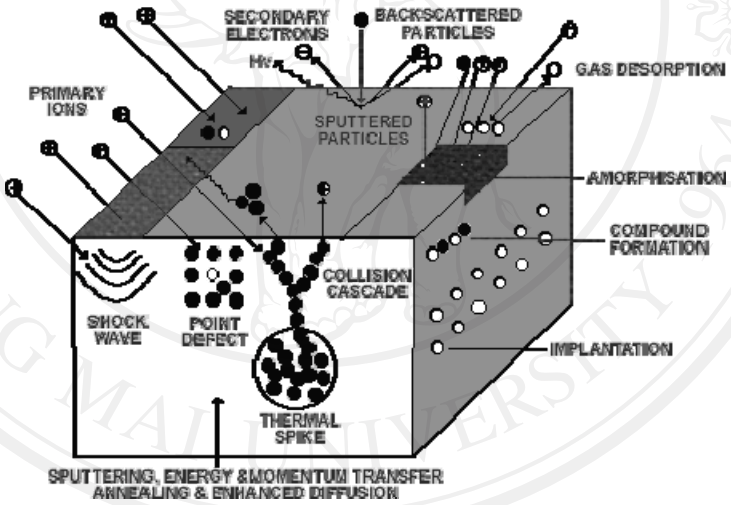

Figure 2.6 Interactions due to ion bombardment (pvd-coatings.co.uk, 2009).

The sputter process has almost no restrictions in the target materials, ranging from pure metals to semiconductors and isolators which require a radio frequency (RF) power supply or pulsed DC. Deposition can be carried out in either non reactive (inert gas only) or reactive (inert & reactive gas) discharges with single or multi-elemental targets.

During the sputter process a magnetic field can be used to trap secondary electrons close to the target. The electrons follow helical paths around the magnetic field lines undergoing more ionizing collisions with neutral gaseous near the target

than would otherwise occur. This enhances the ionization of the plasma near the target leading to a higher sputter rate. It also means that the plasma can be sustained at a lower pressure. The sputtered atoms are neutrally charged and so are unaffected by the magnetic trap. The principle of the sputtering process is shown in Figure 2.7.

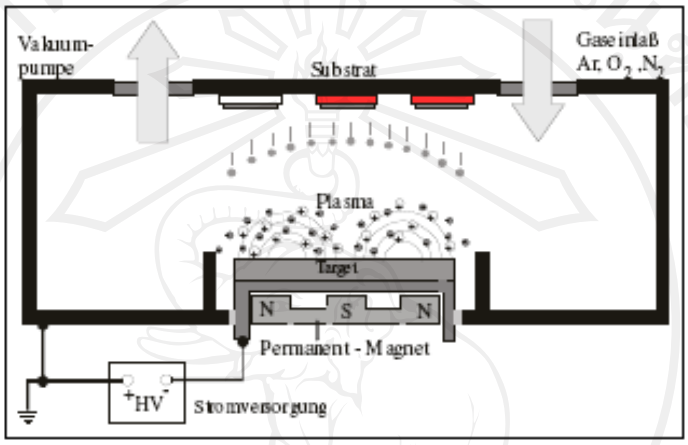

Figure 2.7 The principle of the sputtering process (Institute of Physics of the RWTH Aachen University, 2009).

2.3 Coating characterization and testing

Material characterization and testing are used to indicate the coating structure and properties. This section provides a survey of the coatings characterization and testing used in this research. The diamond and related materials coatings usually analyze for sp^2 and sp^3 structure. Raman spectroscopy is commonly used to identify the I_D and I_G peaks which describe sp^2 and sp^3 ratio. For nitridation and carburization, the glow discharge optical emission spectroscopy (GDOES) was use to specify the atomic distribution depth profile of the treated surface. In addition, the static water contact angle also necessary for fuel cell bipolar plate application. The contact angle and surface energy will consider. The important one is corrosion measurement. The corrosion process and corrosion measurement will be explained. The fuel cell test is

final test for fuel cell performance in this subject. The fuel cell test station would be explained in finally.

2.3.1 Raman spectroscopy

Raman spectroscopy is a spectroscopic technique used in condensed matter physics and chemistry to study vibrational, rotational, and other low-frequency modes in a system. It relies on inelastic scattering, or Raman scattering, of monochromatic light, usually from a laser in the visible, near infrared, or near ultraviolet range. The laser light interacts with phonons or other excitations in the system, resulting in the energy of the laser photons being shifted up or down. The shift in energy gives information about the phonon modes in the system. Typically, a sample is illuminated with a laser beam. Light from the illuminated spot is collected with a lens and sent through a monochromator. Wavelengths close to the laser line, due to elastic Rayleigh scattering, are filtered out while the rest of the collected light is dispersed onto a detector (Raman spectroscopy from wikipedia, 2009).

The scattering of monochromatic radiation that is incident on a sample can tell something of the sample's molecular structure. If the frequency (wavelength) of the scattered radiation is analysed, not only is the incident radiation wavelength observed via elastic scattering (Rayleigh scattering, also accounting for the blue color of the sky), but also a relatively small amount of radiation is scattered inelastically at some different wavelengths, referred to as Stokes and anti-Stokes Raman scattering. Approximately only 1 x 10^{-7} of the scattered light is inelastically scattered Raman. The scattered radiation occurs in all directions and may also have observable changes in its polarization along with its wavelength. The principle of Raman scattering is shown in Figure 2.8.

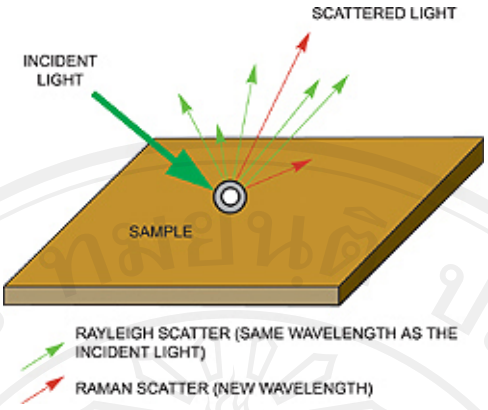

Figure 2.8 Principle of Raman acattering (Andor learning, 2009).

It is the shift in wavelength of the inelastically scattered radiation that provides the chemical and structural information. Raman shifted photons can be of either higher or lower energy, depending upon the vibrational state of the molecule under study. A simplified energy diagram that illustrates these concepts is shown in Figure 2.9.

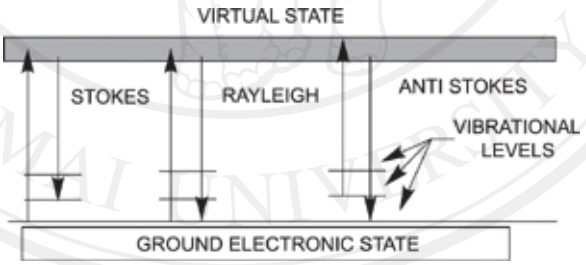

Figure 2.9 Simplified energy diagram (Andor learning, 2009).

Stokes radiation occurs at lower energy (longer wavelength) than the Rayleigh radiation, and anti-Stokes radiation has greater energy. The energy increase or decrease is related to the vibrational energy levels in the ground electronic state of the molecule, and as such, the observed Raman shift of the Stokes and anti-Stokes features are a direct measure of the vibrational energies of the molecule. A schematic Raman spectrum may appear as shown in Figure 2.10.

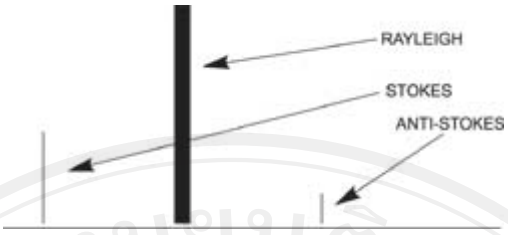

Figure 2.10 Schematic Raman spectrum (Andor learning, 2009).

The energy of the scattered radiation is less than the incident radiation for the Stokes line and the energy of the scattered radiation is more than the incident radiation for the anti-Stokes line. The energy increase or decrease from the excitation is related to the vibrational energy spacing in the ground electronic state of the molecule and therefore the wave number of the Stokes and anti-Stokes lines are a direct measure of the vibrational energies of the molecule.

In the example spectrum, notice that the Stokes and anti-Stokes lines are equally displaced from the Rayleigh line. This occurs because in either case one vibrational quantum of energy is gained or lost. Also, note that the anti-Stokes line is much less intense than the Stokes line. This occurs because only molecules that are vibrationally excited prior to irradiation can give rise to the anti-Stokes line. Hence, in Raman spectroscopy, only the more intense Stokes line is normally measured Raman scattering is a relatively weak process. The number of photons Raman scattered is quite small. However, there are several process which can be used to enhance the sensitivity of a Raman measurement.

2.3.2 Glow discharge optical emission spectroscopy (GDOES)

Glow-discharge optical emission spectrometry (GDOES) is a powerful tool for the rapid analysis of elements in the surface of solids. GDOES can determine quantitatively the bulk concentration of elements in a sample. With further calibration, this technique can describes elemental concentrations as a function of depth into the sample. This allows depth profiling on a host of advanced materials:

treated metals, coated metals and other materials, multi-layers, painted surfaces, hard samples coated with polymers, thin films, and many others.

Emission spectrometry is a well-known technique for analyst an unknown material for the elements present in the sample. When a material is heated sufficiently, it will emit visible light in a discrete spectrum characteristic of the elements in the sample. Each element has its unique atomic emission spectrum (both for visible light and for x-rays). Payling and Larkins (2000) have recently published a new catalogue of atomic spectra for all the elements. Thus if one obtains an atomic spectrum from an unknown sample, he may identify the elements in the sample by comparing the spectrum with those of the elements in the spectral database.

There are three common means of heating the sample to produce the optical emission. The first is to apply a high electrical voltage across the sample, which heats the sample in a spark discharge (arc/spark instruments). Another is to dissolve the sample in acid, and "burn" the solution in an argon plasma (ICP). The third is to sputter the sample surface with argon, and excite the sputtered atoms in the argon plasma (glow discharge). The third heating technique would be discusses.

Figure 2.11 shows a schematic of the glow-discharge lamp. The sample forms the cathode and a thin (2-8 mm diameter) metal tube forms the anode. A small O-ring separates the anode from the cathode. High-purity argon is pumped into the chamber. A high voltage (DC or RF) between sample and anode ionizes the argon to produce a glow discharge. The excited argon ions bombard the sample and cause uniform sputtering of the sample surface. The sputtered atoms from the sample enter the plasma, and they are excited by collisions with electrons or other argon atoms. Those excited atoms from the sample eventually have energy decays to stable states, and the optical emission forms the atomic spectrum from the sample.

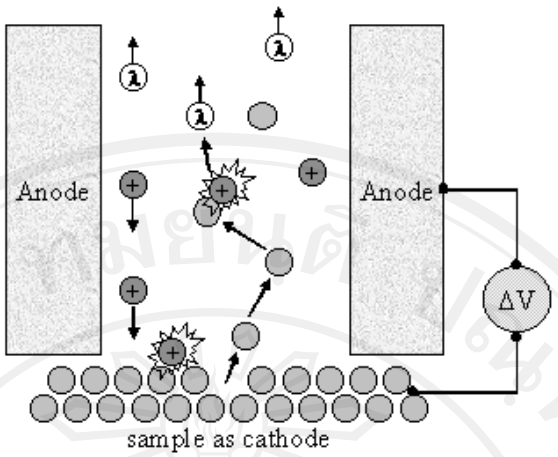

Figure 2.11 Schematic of the glow-discharge lamp and associated process (Long, 2001).

The light emitted by the sample, which is characteristic of the atoms sputtered from the surface, passes through a window into a standard polychromator to be dispersed off a curved, holographic diffraction grating. A series of fixed photomultiplier tubes detect and record specific wavelengths of visible light, corresponding to selected elements.

The applied voltage may be either DC or RF. DC lamps work on conductive samples only. RF lamps are a more recent development in GDOES (Marcus, 1993), and enable the analysis of non-conductive materials. A typical bias voltage is -1000 volts from anode to cathode.

With appropriate calibration one may employ GDOES to determine quantitatively the bulk concentration of elements in a sample. This technique is very common. The signals from the detectors are integrated over the analysis time (1 minute or less for a bulk metal) to yield bulk elemental concentrations. More recent advances in techniques and instrumentation allow the calibration of sputter rate. The glow discharge sputters the sample uniformly, producing a shallow crater in the sample. The plasma sputters a measurable thickness of sample in a given time, on the order of microns per minute in metals. The detectors acquire data very fast, up to 2000 measurements per second for each photomultiplier. Thus a plot of detector

intensity versus time can be transformed through sputter-rate calibrations to a depth profile of elemental concentration versus depth into the sample.

Depending on the standards used and the quality of the calibration, depth may be resolved to 100 nm or less. This allows depth profiling on coated metals and other materials. If an RF glow-discharge source is used, quantitative depth profiling (QDP) on ceramics, polymers, and non-conductive coatings on conductors is possible. QDP analysis by means of an RF source is the recent innovation in GDOES, and is still under development. QDP by a DC source is more established and better understood. Wĕiss and Marshall (1997) introduced that for more information about the fundamental of GDOES can be found in Marcus (1993) and Bogaerst and Rijbels (1997).

2.3.3 Surface energy and contact angle

The definition from Wikipedia (www.wikipedia.org) indicated that Surface energy quantifies the disruption of intermolecular bonds that occurs when a surface is created. In the physics of solids, surfaces must be intrinsically less energetically favorable than the bulk of a material; otherwise there would be a driving force for surfaces to be created, and surface is all there would be. The surface energy may therefore be defined as the excess energy at the surface of a material compared to the bulk. For a liquid, the surface tension (force per unit length) and the surface energy density are identical. Water has a surface energy density of 0.072 J/m^2 and a surface tension of 0.072 N/m.

Cutting a solid body into pieces disrupts its bonds, and therefore consumes energy. If the cutting is done reversibly (see reversible), then conservation of energy means that the energy consumed by the cutting process will be equal to the energy inherent in the two new surfaces created. The unit surface energy of a material would therefore be half of its energy of cohesion, all other things being equal; in practice, this is true only for a surface freshly prepared in vacuum. Surfaces often change their form away from the simple "cleaved bond" model just implied above. They are found

to be highly dynamic regions, which readily rearrange or react, so that energy is often reduced by such processes as passivation or adsorption.

Surface energy is most commonly quantified using a contact angle. It is the interaction between the forces of cohesion and the forces of adhesion which determines whether or not wetting, the spreading of a liquid over a surface, occurs. If complete wetting does not occur, then a bead of liquid will form, with a contact angle which is a function of the surface energies of the system.

The contact angle is the angle at which a liquid/vapor interface meets the solid surface. The contact angle is specific for any given system and is determined by the interactions across the three interfaces. Most often the concept is illustrated with a small liquid droplet resting on a flat horizontal solid surface. The shape of the droplet is determined by the Young Relation. The contact angle plays the role of a boundary condition. Usually, contact angle is measured using a contact angle goniometer. The contact angle is not limited to a liquid/vapour interface; it is equally applicable to the interface of two liquids or two vapours.

Consider a liquid drop on a solid surface. If the liquid is very strongly attracted to the solid surface (for example water on a strongly hydrophilic solid) the droplet will completely spread out on the solid surface and the contact angle will be close to 0°. Less strongly hydrophilic solids will have a contact angle up to 90°. On many highly hydrophilic surfaces, water droplets will exhibit contact angles of 0° to 30°. If the solid surface is hydrophobic, the contact angle will be larger than 90° . On highly hydrophobic surfaces the surfaces have water contact angles as high as 150° or even nearly 180°. On these surfaces, water droplets simply rest on the surface, without actually wetting to any significant extent. These surfaces are termed superhydrophobic and can be obtained on fluorinated surfaces (Teflon-like coatings) that have been appropriately micropatterned. This is called the Lotus effect, as these new surfaces are based on lotus plants' surface. The contact angle thus directly provides information on the interaction energy between the surface and the liquid.

The theoretical description of contact arises from the consideration of a thermodynamic equilibrium between the three phases: the liquid phase of the droplet (L), the solid phase of the substrate (S), and the gas/vapor phase of the ambient (V)

(which will be a mixture of ambient atmosphere and an equilibrium concentration of the liquid vapor). The V phase could also be another (immiscible) liquid phase. At equilibrium, the chemical potential in the three phases should be equal. It is convenient to frame the discussion in terms of the interfacial energies.

Young's equation as shown in figure 2.12 is used to describe the interactions between the forces of cohesion and adhesion and measure what is referred to as surface energy.

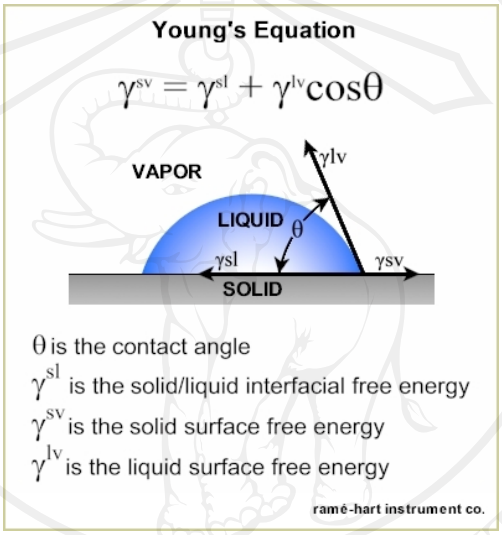

Figure 2.12 A drop of liquid describe Young's equation (Ramehart, 2009).

A drop with a large contact angle is hydrophobic. This condition is exemplified by poor wetting, poor adhesiveness and the solid surface free energy is low. A drop with a small contact angle is hydrophilic. This condition reflects better wetting, better adhesiveness, and higher surface energy. The relation of hydrophobic and hydrophilic drop with there parameters are shown in Figure 2.13.

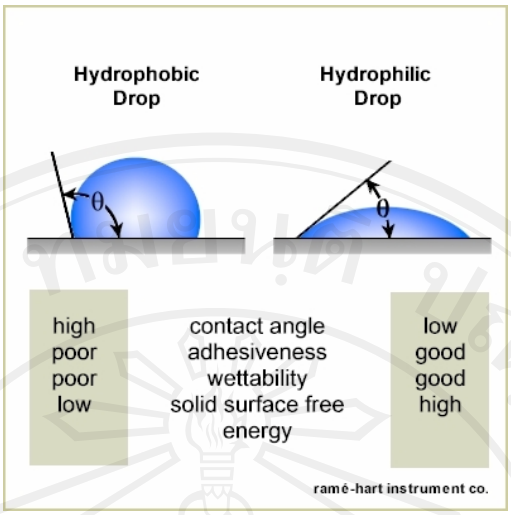

Figure 2.13 Liquid drop of hydrophobic and hydrophilic (Ramehart, 2009).

Contact angle is an invaluable metric for understanding material surface properties; adhesion, wettability, and solid surface free energy. Contact angle is used to measure cleanliness, the effects of surface treatments, adhesiveness, repellency. In the improvement of bipolar plate surface, contact angle is used to characterized the hydrophobic of its surface. In the operation of PEM fuel cell, too much water may cause flooding in either the catalyst layer or the gas diffusion layer or even in the gas channels. The result of cell flooding is loss of cell potential due to difficulty of one or both reactant gases reaching the catalyst sites. But, too little water is likely to cause membrane drying, which is turn increases cell resistance and reduces cell potential.

2.3.4 Corrosion measurement

Most metal corrosion occurs via electrochemical reactions at the interface between the metal and an electrolyte solution. Corrosion normally occurs at a rate determined by an equilibrium between opposing electrochemical reactions. The first is the anodic reaction, in which a metal is oxidized, releasing electrons into the metal. The other is the cathodic reaction, in which a solution species (often O_2 or H^+) is reduced, removing electrons from the metal. When these two reactions are in equilibrium, the flow of electrons from each reaction is balanced, and no net electron

flow (electrical current) occurs. The two reactions can take place on one metal or on two dissimilar metals (or metal sites) that are electrically connected.

Figure 2.14 diagrams this process. The vertical axis is potential and the horizontal axis is the logarithm of absolute current. The theoretical current for the anodic and cathodic reactions are shown as straight lines. The curved line is the total current; the sum of the anodic and cathodic currents. This is the current that you measure when you sweep the potential of the metal with your potentiostat. The sharp point in the curve is actually the point where the current changes signs as the reaction changes from anodic to cathodic, or vice versa. The sharp point is due to the use of a logarithmic axis. The use of a log axis is necessary because of the wide range of current values that must be displayed during a corrosion experiment. Because of the phenomenon of passivity, it is not uncommon for the current to change by six orders of magnitude during a corrosion experiment.

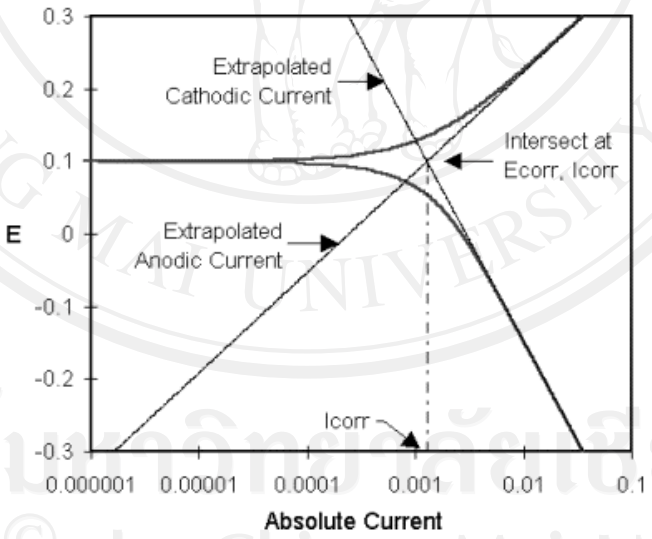

Figure 2.14 Corrosion Process Showing Anodic and Cathodic Current Components with Classic Tafel Analysis (Gamry instruments, 2009).

The potential of the metal is the means by which the anodic and cathodic reactions are kept in balance. Refer to figure 2.14. Notice that the current from each half reaction depends on the electrochemical potential of the metal. Suppose the

anodic reaction releases too many electrons into the metal. Excess electrons shift the potential of the metal more negative, which slows the anodic reaction and speeds up the cathodic reaction. This counteracts the initial perturbation of the system.

The equilibrium potential assumed by the metal in the absence of electrical connections to the metal is called the Open Circuit Potential, Eoc. In most electrochemical corrosion experiments, the first step is the measurement of Eoc.

The value of either the anodic or cathodic current at Eoc is called the Corrosion Current, Icorr. If we could measure Icorr, we could use it to calculate the corrosion rate of the metal. Unfortunately, Icorr cannot be measured directly. However, it can be estimated using electrochemical techniques. In any real system, Icorr and Corrosion Rate are a function of many system variables including type of metal, solution composition, temperature, solution movement, metal history, and many others.

In practice, many metals form an oxide layer on their surface as they corrode. If the oxide layer inhibits further corrosion, the metal is said to passivate. In some cases, local areas of the passive film break down allowing significant metal corrosion to occur in a small area. This phenomena is called pitting corrosion or simply pitting.

Because corrosion occurs via electrochemical reactions, electrochemical techniques are ideal for the study of the corrosion processes. In electrochemical studies, a metal sample with a surface area of a few square centimeters is used to model the metal in a corroding system. The metal sample is immersed in a solution typical of the metal's environment in the system being studied. Additional electrodes are immersed in the solution, and all the electrodes are connected to a device called a potentiostat. A potentiostat allows you to change the potential of the metal sample in a controlled manner and measure the current flows as a function of potential.

Both controlled potential (potentiostatic) and controlled current (galvanostatic) polarization is useful. When the polarization is done potentiostatically, current is measured, and when it is done galvanostatically, potential is measured. This discussion will concentrate on controlled potential methods, which are much more

common than galvanostatic methods. With the exception of Open Circuit Potential vs. Time, Electrochemical Noise, Galvanic Corrosion, and a few others, potentiostatic mode is used to perturb the equilibrium corrosion process. When the potential of a metal sample in solution is forced away from Eoc, it is referred to as polarizing the sample. The current of the metal sample is measured as it is polarized. The response is used to develop a model of the sample's corrosion behavior.

Suppose we use the potentiostat to force the potential to an anodic region (towards positive potentials from Eoc). In Figure 2.14, we are moving towards the top of the graph. This will increase the rate of the anodic reaction (corrosion) and decrease the rate of the cathodic reaction. Since the anodic and cathodic reactions are no longer balanced, a net current will flow from the electronic circuit into the metal sample. The sign of this current is positive by convention. If we take the potential far enough from Eoc, the current from the cathodic reaction will be negligible, and the measured current will be a measure of the anodic reaction alone. In Figure 2.14, notice that the curves for the cell current and the anodic current lie on top of each other at very positive potentials. Conversely, at strongly negative potentials, cathodic current dominates the cell current.

In certain cases as we vary the potential, we will first passivate the metal, then cause pitting corrosion to occur. With the astute use of a potentiostat, an experiment in which the current is measured versus potential or time may allow us to determine Icorr at Ecorr, the tendency for passivation to occur, or the potential range over which pitting will occur.

Classic Tafel analysis is performed by extrapolating the linear portions of a log current versus potential plot back to their intersection, see Figure 2.14. The value of either the anodic or the cathodic current at the intersection is Icorr. However, many real world corrosion systems do not provide a sufficient linear region to permit accurate extrapolation. The modern corrosion test software, such as SoftCorr III software, performs a numerical fit for Icorr and calculate corrosion rate.

Calculation of Corrosion Rate from Corrosion Current

The numerical result obtained by fitting corrosion data to a model is generally the corrosion current. We are interested in corrosion rates in the more useful units of rate of penetration, such as millimeters per year. How is corrosion current used to generate a corrosion rate? Assume an electrolytic dissolution reaction involving a chemical species, S:

$$S \rightarrow S^{n+} + ne^{-} \quad . \tag{2.12}$$

You can relate current flow to mass via Faraday's Law.

$$Q = n F M \quad , \tag{2.13}$$

where

Q is the charge in coulombs resulting from the reaction of species S
n is the number of electrons transferred per molecule or atom of S
F is Faraday's constant = 96,486.7 coulombs/mole
M is the number of moles of species S reacting

A more useful form of equation (2.13) requires the concept of equivalent weight. The equivalent weight (EW) is the mass of species S that will react with one Faraday of charge. For an atomic species, EW = AW/n (where AW is the atomic weight of the species).

Recalling that M = W/AW and substituting into equation (2.13) we get:

$$W = EW\ Q\ /\ F \quad , \tag{2.14}$$

where W is the mass of species S that has reacted.

In cases where the corrosion occurs uniformly across a metal surface, the corrosion rate can be calculated in units of distance per year. Be careful, this calculation is only valid for uniform corrosion, it dramatically underestimates the problem when localized corrosion occurs!

For a complex alloy that undergoes uniform dissolution, the equivalent weight is a weighted average of the equivalent weights of the alloy components. Mole fraction, not mass fraction, is used as the weighting factor. If the dissolution is not uniform, we may have to measure the corrosion products to calculate EW.
Conversion from a weight loss to a corrosion rate (CR) is straightforward. We need to know the density, d, and the sample area, A. Charge is given by Q = I T, where T is the time in seconds and I is a current. We can substitute in the value of Faraday's constant, M.

By modifying equation (2.14):

$$CR = Icorr\ K\ EW\ /\ d\ A \qquad (2.15)$$

Where

CR The corrosion rate. Its units are given by the choice of K (see table 2.1)

Icorr The corrosion current in amps

K A constant that defines the units for the corrosion rate

EW The equivalent weight in grams/equivalent

d Density in grams/cm^3

A Sample area in cm^2

Table 2.1 shows the value of K used in equation (2.15) for corrosion rates in the units of your choice.

Table 2.1 Corrosion rate constants (Gamry instrument, 2009).

Corrosion Rate Units	**K**	**Units**
mm/year (mmpy)	3272	mm/(amp-cm-year)
millinches/year (mpy)	1.288×10^5	milliinches(amp-cm-year)

Several electrochemical techniques have been approved by the ASTM (American Society for Testing and Materials, 100 Barr Harbor Drive, West Conshohocken, PA 19428, www.astm.org). They may be found in Volume 3.02 of the ASTM Standards such as G 5: Potentiostatic and Potentiodynamic Anodic Polarization Measurements. For further information about corrosion, see Uhlig and Revie (1985).

2.3.5 Fuel cell test station

The fuel cell test station compose of electric and gas circuit accessories on a stand board, gases humidifiers and computer control system. Fuel cell control, data acquisition and analysis system has been designed by Michael Rhodes (Institute for Science and Technology Research and Development). The entire control system is completely contained in a small footprint box that can fit on a desktop allowing it to be portable, including the ability to be controlled by a desktop computer or a laptop computer.

The system consists of a single circuit board, designed and built in-house, with a central PIC microcontroller as the primary intelligence. The board also contains a 16-channel 12-bit analog to digital converter (ADC), 4-channel 12-bit digital to analog (DAC) converter, 5 general purpose digital I/O ports for the MFC, and 8 solid state relay (SSR) drivers for heater control. The ADC is used to read the pressure sensors, temperature sensors and the mass flow controller flow rate. The present configuration supports 6 pressure transducers (voltage or 4-20mA current loop types), 6 temperature sensors, 2 mass flow controllers, electronic load current/voltage monitoring channels and 8 solid state relays for heater control.

The sensitivity of each sensor type is .0244 psi out of a range of 100 psi for the pressure sensors, .122 sccm out of a range of 500 sccm for the mass flow controller, .1°C out of a range of 100 ºC for the temperature sensors, and 30mV/30mA for the electronic load out of a range of 120V/120A. The ADC for the electronic load current and voltage monitor will be upgraded shortly to an 18-bit ADC allowing for a

resolution of .5mv and.5mA respectively. This new ADC was also designed and built in-house.

Communication to the electronic load is by way of a USB GPIB interface connected to a PC while communication to the main controller is through a RS232 (com port) on the PC. This allows easy transition of the control system from one computer to another including laptop computers allowing portability of the entire system.

Two programming environments were used to develop the software. The first was PIC Basic Pro used to program the PIC microprocessor and Visual Basic for the main PC side operator control and graphical user interface. When running the control program the operator is presented with a screen that is similar to a process control environment. This includes analog style gauges for pressure, mass flow rate, voltage, current, power and temperature. These are supplemented with the digital values for more precise interpretation of the values. Analog gauges where used due to the fact that rates of change are more easily identified then with their digital equivalents.

Continuous runtime updates for the electronic load parameters are presented in a standard moving chart recorder on screen. This includes the voltage, current and power of the load. A second graphing window with real-time update is current density plots. This displays the current density in mA/cm^2 versus voltage and current density in mA/cm^2 versus power. Other features of the program allows ramping of any of the dependent variables such as ramping down the resistance over a period of time, ramping temperatures and ramping flow rates allowing the operator to further characterize the fuel cell. The diagram of the fuel cell control system shown in Figure 2.15.

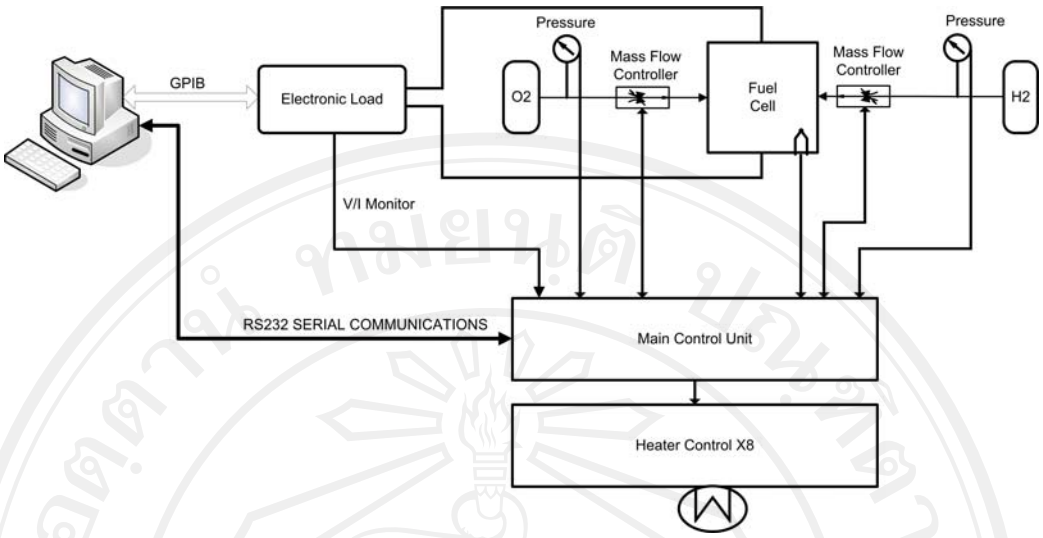

Figure 2.15 Diagram of the fuel cell control system designed by Michael Rhodes.

Fuel cell performance is characterized by its polarization curve, a plot of cell potential and current density. However, in practice, the open circuit potential is significantly lower than the theoretical potential. This suggests that there are some losses in the fuel cell even when no external current is generated. When the fuel cell connected with a load, the potential is expected to drop even further as a function of current being generated, due to unavoidable losses. Consider the polarization curve, there are three distinct regions are noticeable as shown in Figure 2.16.

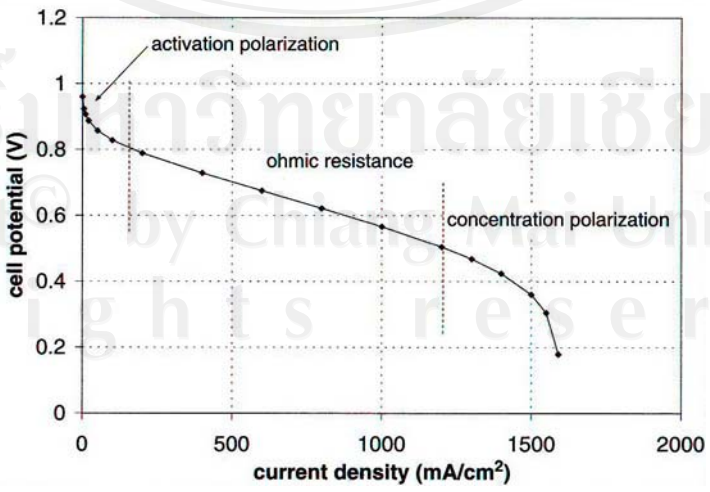

Figure 2.16 A fuel cell polarization curve with three distinct regions (Barbir, 2005).

A common method to determine cell voltage losses is least squares fitting of an analytical expression incorporating the three main sources of loss to the experimental performance data. The voltage losses for each region caused by;

- At low current density, the cell potential drops sharply as a result of the activation polarization.

- At intermediate current density, the cell potential drops linearly with current; clearly as a result of ohmic losses (i.e., cell resistance).

- At high current densities, the cell potential drop depart from linear relationship with current density, as a result of more pronounced concentration polarization.

By fitting the experimental results to the equations describing the polarization curve (Barbir, 2005);

$$E_{cell} = E_{r,T,P} - \frac{RT}{\alpha F}\ln\left(\frac{i+i_{loss}}{i_0}\right) - \frac{RT}{nF}\ln\left(\frac{i_L}{i_L - i}\right) - iR_i \qquad (2.16)$$

Insightful information may be gained about the parameters of the polarization curve, such as reversible cell potential, V_r ; apparent exchange current density, i_0 ; Tafel slope, b; cell resistance, R_i ; or limiting current, i_L.

Some information of the parameters gave as follow;

$E_{r,T,P}$ is reversible potential at temperature T and pressure P. E_r described reversible or equilibrium potential. The reversible potential at the fuel cell anode is 0 V by definition, and the reversible potential at the fuel cell cathode is 1.229 V (at 25 ºC and atmospheric pressure). The difference between the electrode potential and the reversible potential is called over potential. It is the potential difference required to generate current.

R and T are gas constant (8.314 J $mole^{-1}$ K^{-1}) and temperature (K) respectively.

α is transfer coefficient. The transfer coefficient for hydrogen/oxygen fuel cell using Pt catalyst have value around 1.

n and F are number of electron involved and Faraday's constant (96,485 C $mole^{-1}$) respectively. On the anode side n = 2, and on the cathode side n = 4.

i is current density (A cm^{-2}). The surface concentration reach zero when the rate of consumption exceeds the diffusion rate; the reactant is consumed faster than it can reach the surface. Current density at which this happens is called the limiting current density (i_L). A fuel cell cannot produce more than the limiting current because there are no reactants at the catalyst surface.

At equilibrium, the potential is E_r, and the net current is equal to zero, although the reaction proceeds in both directions is simultaneously. The rate at which these reaction proceed at equilibrium is called the exchange current density (i_0). Exchange current density is a measure of an electrode's readiness to proceed with the electrochemical reaction. If the exchange current density is high, the surface of the electrode is more active.

The cell resistance (R_i) is total cell internal resistance which includes ionic, electronic, and contact resistance (Ω cm^2).